Inorganic Chemistry

Article

pubs.acs.org/IC

Functionalized Defects through Solvent-Assisted Linker Exchange: Synthesis, Characterization, and Partial Postsynthesis Elaboration of a Metal–Organic Framework Containing Free Carboxylic Acid Moieties

Olga Karagiaridi,[†] Nicolaas A. Vermeulen,[†] Rachel C. Klet,[†] Timothy C. Wang,[†] Peyman Z. Moghadam,[‡] Salih S. Al-Juaid,[§] J. Fraser. Stoddart,*[,†] Joseph T. Hupp,*[,†] and Omar K. Farha*[,†,§]

[†]Department of Chemistry and International Institute for Nanotechnology and [‡]Department of Chemical and Biological Engineering, Northwestern University, 2145 Sheridan Road, Evanston, Illinois 60208, United States

[§]Department of Chemistry, Faculty of Science, King Abdulaziz University, Jeddah, Saudi Arabia

Supporting Information

ABSTRACT: Intentional incorporation of defect sites functionalized with free carboxylic acid groups was achieved in a paddlewheel-based metal–organic framework (MOF) of **rht** topology, **NU-125**. Solvent-assisted linker exchange (SALE) performed on a mixed-linker derivative of **NU-125** containing isophthalate (**IPA**) linkers (**NU-125-IPA**) led to the selective replacement of the **IPA** linkers in the framework with a conjugate base of trimesic acid (**H_3BTC**). Only two of the three carboxylic acid moieties offered by **H_3BTC** coordinate to the Cu_2 centers in the MOF, yielding a rare example of a MOF decorated with free −COOH groups. The presence of the −COOH groups was confirmed by diffuse reflectance infrared Fourier-transformed spectroscopy (DRIFTS); moreover, these groups were found to be available for postsynthesis elaboration (selective monoester formation). This work constitutes an example of the use of SALE to obtain otherwise challenging-to-synthesize MOFs. The resulting MOF, in turn, can serve as a platform for accomplishing selective organic transformations, in this case, exclusive monoesterification of trimesic acid.

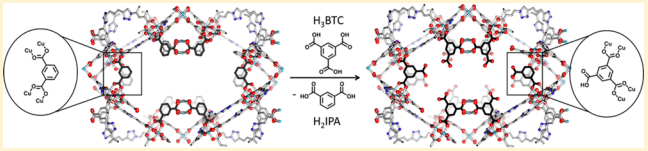

INTRODUCTION

Hybrid materials that combine the rigidity of inorganic compounds with the flexibility and the tunability of organic matter are attractive candidates for several industrially relevant tasks, including new tasks pertaining to alternative energy and sustainability. It is hardly surprising, therefore, that the emerging class of porous hybrid materials known as metal–organic frameworks (MOFs)[1] has generated an impressive amount of research over the past two decades. MOFs have been studied as promising candidates for, among other things, gas storage,[2−4] separation,[5−7] catalysis,[8−10] sensing,[11] toxic gas removal,[12,13] and light harvesting.[14−16]

Despite the fact that by definition MOFs are highly modular hybrid materials (composed of metal-based nodes connected by organic linkers, with a large variety of structural building blocks available for the synthesis of "tailor-made" products), taking advantage of their signature tailorability is not always straightforward.[17−19] In particular, incorporation of reactive organic functionalities into MOF cages has proven to be a formidable task, as these moieties tend to react with the MOF metal precursors under the solvothermal conditions typically employed to synthesize MOFs rather than remain free to be harnessed for further application. This complication is particularly relevant for the incorporation of free carboxylic acid groups. Carboxylates form relatively strong coordination bonds with the MOF metal centers and are therefore commonly employed as MOF linkers. To prevent unwanted coordination of carboxylates to metal nodes, several strategies have been employed, including reliance on the steric demands of the framework,[20,24] variation of synthetic conditions (choice of solvent,[21] synthesis in the absence of bases,[22] or use of acidic conditions[23]), and postsynthesis deprotection.[25] Nevertheless, the overall number of reports outlining the successful, intentional incorporation of free carboxylic acid groups into MOFs remains small. Since free carboxylic acid-containing MOFs are anticipated to have great utility in a range of applications (including organocatalysis, enhancement of proton conductivity, and capture of vapor-phase ammonia[26]), the array of methods available for their synthesis merits expansion and diversification.

Recently, solvent-assisted linker exchange (SALE) has been shown to be remarkably versatile and effective for the synthesis of MOFs that are difficult to access de novo (i.e., through a one-pot solvothermal reaction).[27−42] Briefly, SALE involves replacing the linkers in a parent metal–organic framework with linkers of choice (e.g., functionalized linkers,[29] linkers that can serve as a catalyst precursor,[30] longer linkers[36]) via a

Received: November 10, 2014
Published: January 29, 2015

DOI: 10.1021/ic502697y
Inorg. Chem. 2015, 54, 1785−1790

Scheme 1. Idealized Representation of the Synthesis of NU-125-HBTC by SALE of IPA for HBTC in NU-125-IPA

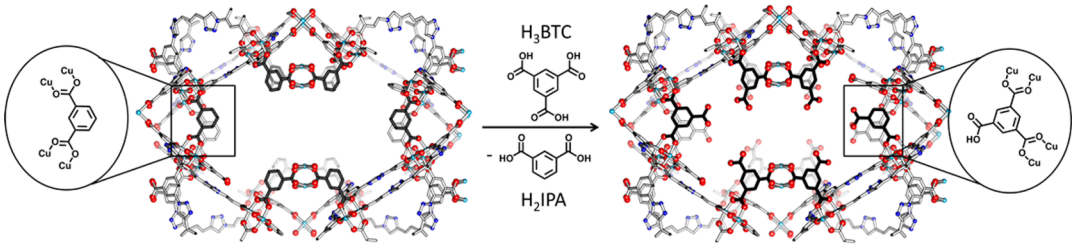

heterogeneous reaction in a carefully selected solvent.[27,28] We hypothesized that SALE would be an effective method for obtaining MOFs featuring free (i.e., linker-pendant, rather than node-coordinated) carboxylic acid moieties. Relevant to this goal, we[43] and others[44] have reported on intentional introduction of structural defects (e.g., missing phenyl carboxylate fragments) into copper-paddlewheel-based MOFs. Barin et al. showed that it was possible to incorporate defects into the framework of **NU-125** (**Cu_3L**),[45] a highly porous paddlewheel-based MOF of **rht** topology that features as a linker the fully deprotonated conjugate base of 5,5′,5″-(4,4′,4″-(benzene-1,3,5-triyl)tris(1*H*-1,2,3-triazole-4,1-diyl))-triisophthalic acid (**H_6L**).[43] Synthesis of **NU-125** in the presence of diacid linker precursors, such as isopthalic acid (**H_2IPA**), led to framework incorporation of **IPA** and associated node vacancies, in lieu of **L**. The resulting structural defects (voids) significantly alter the material's textural properties as shown by augmentation of the Brunauer–Emmett–Teller (BET) area and the pore volume. Herein, we apply SALE to a sample of **NU-125** featuring **IPA** defects to selectively replace the diacid molecules with a monoprotonated conjugate base of benzene-1,3,5-tricarboxylic acid (**H_3BTC**, Scheme 1). The **rht** topology of **NU-125** in combination with the steric demands of the framework allows the **H_3BTC** molecules to coordinate to the Cu_2 centers using only two of the three carboxylic acid groups, resulting in the functionalization of the defect voids with free carboxylic acid moieties (one per added **BTC** unit) as shown in Scheme 1. The porosity and crystallinity of the framework is preserved, and the presence of free carboxylic acid moieties was confirmed by diffuse reflectance infrared Fourier-transformed spectroscopy (DRIFTS). Additionally, we found that the free carboxylic acid groups can be elaborated, without damage to surrounding moieties. Thus, reaction of **NU-125** containing **HBTC** defects with trimethylsilyldiazomethane (TMS–CHN_2) culminates in selective methylation of only the free carboxylic acid group of the **HBTC** linkers, resulting in the selective synthesis of the monomethyl ester of **BTC** (within the MOF) or **H_3BTC** (once released from the MOF).

RESULTS AND DISCUSSION

Synthesis of NU-125-HBTC. Initially, incorporation of **HBTC** defects into **NU-125** was attempted in a similar fashion to the de novo method that was reported by Barin et al. Following the procedure established by the authors, **NU-125** was synthesized at 80 °C in the presence of **H_3BTC**, utilizing the reported optimal **H_6L:H_3BTC** feed ratio of 1:3. A blue crystalline powder was obtained, and its powder X-ray diffraction (PXRD) pattern resembles that of **NU-125** in terms of peak positions but differs from it in terms of peak intensities (the peak at 2θ = 5.35 exhibits a much elevated intensity compared to the corresponding peak in the simulated pattern of **NU-125**; Figure S13, Supporting Information). The ^{1}H NMR spectrum of the digested **BTC**-functionalized product indicated the presence of **BTC** in the powder with the **L:BTC** ratio of 1:2 (Figure S3, Supporting Information). However, scanning electron microscopy (SEM) images of the powder revealed the absence of the characteristic octahedral crystals associated with the **rht** topology of **NU-125** (Figure 1). Instead, an agglomerated and likely polycrystalline phase was observed on top of a large amount of possibly amorphous plates (Figure 1a). Furthermore, upon activating the material by solvent exchange to ethanol (EtOH), supercritical CO_2 drying[46,47] and heating under vacuum to remove solvent molecules coordinated to the Cu_2 centers, and collecting its N_2 isotherm, it was discovered that the material did not possess the exceptional porosity of **NU-125** (~3000 m^2/g), as its BET area was only 470 m^2/g (Figure 1c). The PXRD, SEM, and N_2 sorption data together suggest that the de novo synthesized material is not isostructural with **NU-125** and that defect incorporation takes place in a different manner from that observed in the published **IPA**-functionalized material (**NU-125-IPA**).

To achieve the desired **HBTC** incorporation into **NU-125**, we turned to SALE. We synthesized the **NU-125** analogue featuring **IPA** defects using a previously optimized **H_6L:H_2IPA** feed ratio of 1:3. The resulting product, hereafter referred to as **NU-125-IPA**, possesses a **L:IPA** ratio of 1:1, as indicated by ^{1}H NMR spectroscopy, and is isostructural with **NU-125** according to its PXRD pattern (Figures S1 and S13, Supporting Information). After being soaked in *N*,*N*-dimethylformamide (DMF), **NU-125-IPA** was subjected to SALE with 3 equiv of **H_3BTC** at 80 °C overnight. The ^{1}H NMR spectrum of the product **NU-125-HBTC** showed complete replacement of the **IPA** linkers with **BTC**, while the **L**:defect ratio remained 1:1 (Figure S4, Supporting Information). No leaching of **L** linkers into the solution took place during the SALE reaction, as evidenced by ^{1}H NMR spectroscopy of the evaporated (and redissolved) reaction solution, even when increased amounts of **IPA** were used or when the reaction was allowed to run for more than 48 h (Figure S6, Supporting Information). The PXRD pattern of **NU-125-HBTC** confirms isostructurality with **NU-125**, matching well with the simulated pattern of **NU-125**, in terms of both peak positions and intensities (Figure S13, Supporting Information).

Remarkably, in contrast to the de novo synthesized product, the SEM images of the SALE-obtained **NU-125-HBTC** clearly showed the presence of a single phase composed of well-formed octahedral crystals varying in diameter from 2 to 5 μm (Figure 1b). After the material was activated, N_2 isotherm measurements revealed a BET area of 3030 m^2/g, providing further evidence that the **NU-125-HBTC** material obtained through SALE is structurally similar to **NU-125-IPA** (Figure 1c). Taking into account the **L:BTC** ratio of 1:1 as shown by ^{1}H NMR measurements along with the fact that each hexa-

DOI: 10.1021/ic502697y
Inorg. Chem. 2015, 54, 1785–1790

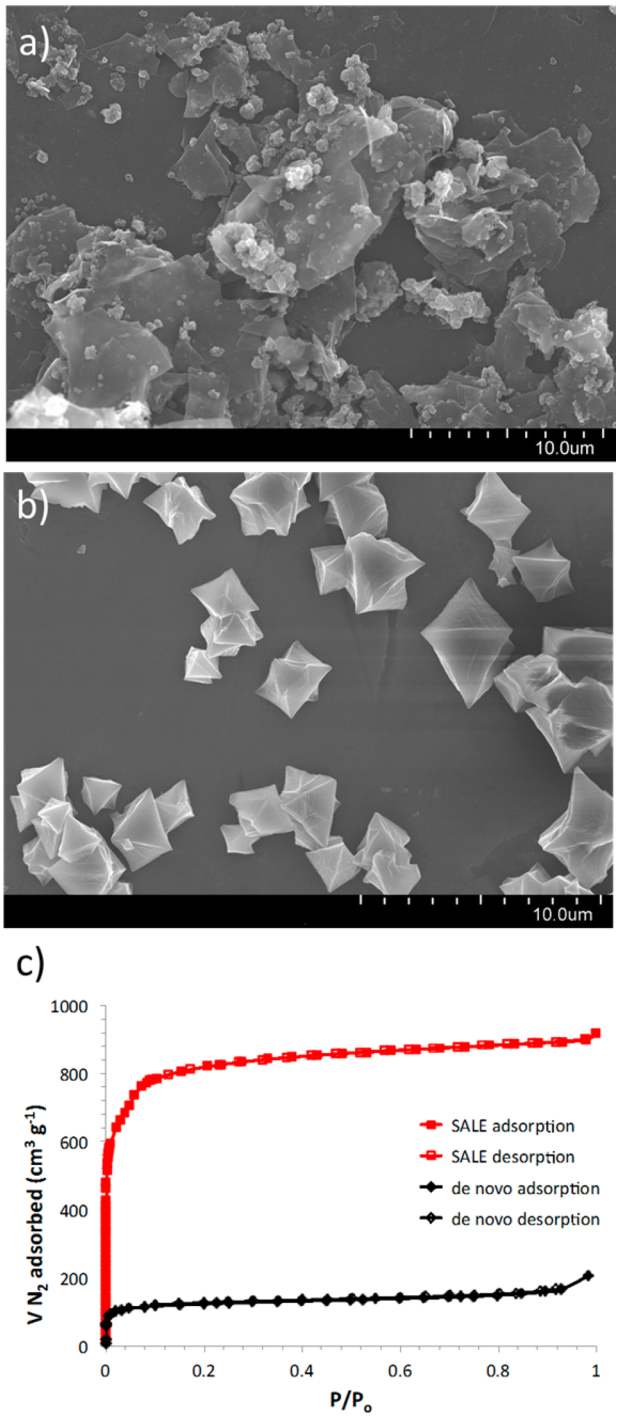

Figure 1. (a) SEM images of the products of the de novo attempt to synthesize **NU-125-HBTC** and (b) the product of SALE of HBTC into **NU-125-IPA**. (c) N_2 isotherms of the products resulting from the de novo and the SALE attempts to synthesize **NU-125-HBTC**.

anionic **L** linker is replaced by three **HBTC** linkers to achieve the expected defect configuration, the proposed formula for **NU-125-HBTC** is $Cu_3L_{0.75}(HBTC)_{0.75}$.

Detection of Free Carboxylic Acid Groups in NU-125-HBTC through DRIFTS Experiments. In search of corroborative (or not) evidence for the proposed SALE-based defect incorporation model (leading to the presence of one free carboxylic acid group per **HBTC** linker) we initially considered ^{1}H NMR spectroscopy. Unfortunately, since solution spectra of the digested MOF are collected in a medium that contains D_2SO_4, labile protons, such as those of the free −COOH groups, cannot be detected. In other words, ^{1}H NMR spectra of the digested crystals can only confirm incorporation of **BTC** linkers, without providing any information regarding their mode of coordination to the Cu_2 centers.

To elicit the needed information we resorted to diffuse reflectance infrared Fourier-transformed spectroscopy (DRIFTS). Notably, DRIFTS is nondestructive, so it can be directly applied to the intact MOF. DRIFTS allows differentiation between coordinated and noncoordinated carboxylate and carboxylic acid moieties, since the vibration associated with the COO−H bond stretch of a free carboxylic acid group exhibits a characteristic band position. Furthermore, DRIFTS can be performed in a dry and air-free atmosphere by using a Praying Mantis cell, thereby ensuring that the integrity of the activated framework is preserved and that no solvent (e.g., H_2O) molecules are coordinated to the free Cu_2 centers.

DRIFTS spectra of both **NU-125-IPA** and **NU-125-HBTC** were collected and compared. Two important differences were observed (Figure 2). The spectrum of **NU-125-HBTC** exhibits

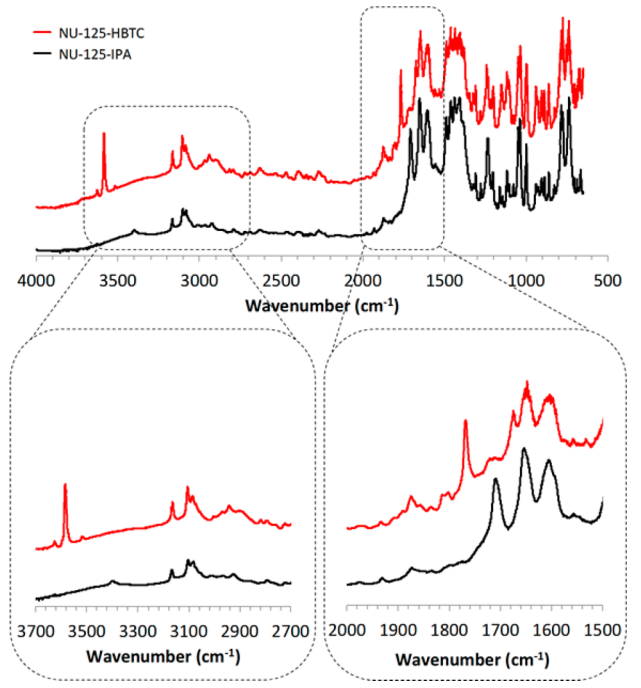

Figure 2. Full DRIFTS spectra of **NU-125-IPA** and **NU-125-HBTC** (black and red, respectively) and highlights of the spectral regions for the non-hydrogen bonding carboxylic acid O−H stretch (2700−3700 cm^{-1}) and the carbonyl stretch of free carboxylic acids (1500−2000 cm^{-1}).

bands at 1750 and 3600 cm^{-1} that are absent from the spectrum of **NU-125-IPA**. As noted in previous work, the band at 1750 cm^{-1} corresponds to the carbonyl stretch of a free −COOH group.[25] The very sharp band at 3600 cm^{-1} elicits a more intriguing interpretation. From tabulated data of infrared absorption frequencies one might naively expect to observe for the O−H stretch of the −COOH group a broad band at 2500−3300 cm^{-1}. These data, however, correspond to nonporous samples, in which neighboring carboxylic acid molecules are able to engage in hydrogen bonding (which leads to band broadening). In contrast, the IR spectrum of vaporized benzoic

DOI: 10.1021/ic502697y
Inorg. Chem. 2015, 54, 1785−1790

acid (with absence of hydrogen bonding) features a sharp band at 3600 cm^{-1}, similar in shape to that observed in the spectrum of **NU-125-HBTC**.[48] The observed similarity is consistent with the proposed model of defect incorporation into the **NU-125** framework, which suggests site isolation of the **HBTC** molecules and precludes hydrogen bonding. The DRIFTS spectrum, therefore, provides strong evidence for the presence of free carboxylic acid moieties inside the framework of **NU-125-HBTC**.

Postsynthesis Methylation of NU-125-HBTC. In order to investigate the availability of the free carboxylic acid moieties for postsynthesis chemical elaboration inside the MOF framework, we attempted an esterification reaction. We reasoned that the results of such an experiment could provide additional evidence for the presence (or not) of the proposed free −COOH groups. Additionally, such results could provide an attractive route for selective monomethylation of **H_3BTC**, since the Cu_2 centers of the paddlewheel structural building units in **NU-125** essentially act as protecting groups for two of the three −COOH functionalities of the **HBTC** molecule.

Methylation of **HBTC** to form the methyl ester **Me-BTC** was achieved by subjecting activated **NU-125-HBTC** to 2 equiv of TMS-CHN_2 in a toluene−methanol solution (2:1 toluene/MeOH v/v) at 0 °C (Figure 3). A ^{1}H NMR spectrum in a d_6-dimethyl sulfoxide-D_2SO_4 solution of crystals that had been subjected to the reaction for 24 h revealed a new peak at 3.85 ppm, indicating the presence of a methyl ester group (Figure S7, Supporting Information). The relative integration of the peak did not change upon extensive solvent exchange of the crystals to EtOH and activation by supercritical CO_2 drying, thus demonstrating that the monomethylated **Me-BTC** units remain part of the framework (Figure S8, Supporting Information). The extent of the methylation, as determined by ^{1}H NMR, was 30−50%. Attempts to achieve more extensive methylation by subjecting the framework to larger amounts of TMS−CHN_2 resulted in partial degradation of the Cu_2 sites (observed by the evolution of black particles—most likely, Cu nanoparticles—upon addition of excessive methylating agent) and subsequent multiple methylation of released **BTC**, as evidenced by ^{1}H NMR data.

The partially methylated **NU-125-Me-BTC** product retained its crystallinity, yielding a PXRD pattern that matched that of its parent to an excellent degree (Figure S14, Supporting Information). The material was activated for N_2 sorption studies by supercritical CO_2 drying without further thermal activation, since monomethylated **H_3BTC** was found to be thermally sensitive; this activation method leaves residual coordinated EtOH molecules. The material is still highly porous, as illustrated by its large BET area (2050 m^2/g; see Figure S20, Supporting Information; for comparison, the BET area of an **NU-125-IPA** sample that had been activated by a similarly mild protocol was 2400 m^2/g). Furthermore, thermogravimetric analysis (TGA) data suggest that the three materials (**NU-125-IPA**, **NU-125-HBTC**, and **NU-125-Me-BTC**) have similar thermal stabilities (with thermal decomposition occurring around 300 °C).

In order to quantify the extent of **HBTC** methylation as well as to confirm the selectivity of the reaction, we utilized high-performance liquid chromatography (HPLC). Analysis by HPLC requires that the diacid linkers be removed from the MOF framework and dissolved in a suitable solution medium. Conveniently, SALE provides a facile route for the realization of this goal, as the **HBTC** and **Me-BTC** linkers inside **NU-125-Me-BTC** can be replaced by **IPA** due to the small difference in the pK_a of these diacids (Figure 3). Prior to SALE, the TMS-CHN_2-treated MOF was extensively solvent exchanged with EtOH to ensure complete removal of the methylating agent and then activated via supercritical CO_2 drying. The material was then subjected to SALE with **IPA** in DMF. After 24 h, an aliquot of the SALE solution was removed from the reaction vessel, the solvent was removed in vacuo, and the solid residue was dissolved in an appropriate HPLC solvent and analyzed by HPLC (see Supporting Information for details). Figure 3 shows the HPLC elution profile of the sample as well as elution profiles of relevant molecular standards (**H_2IPA, H_3BTC**, and mono-, di-, and trimethyl esters of **H_3BTC**) and samples of **NU-125-IPA** and **NU-125-HBTC** (see Supporting Information for sample preparation details). From the elution profiles, it is evident that the only species present in the trace corresponding to **NU-125-Me-BTC** are **H_3BTC**, **H_2BTC-Me**, and **H_2IPA** (present in excess in the SALE solution); no di- or trimethyl ester products are observed, illustrating the selectivity of the reaction. Mass spectra collected on the sample further

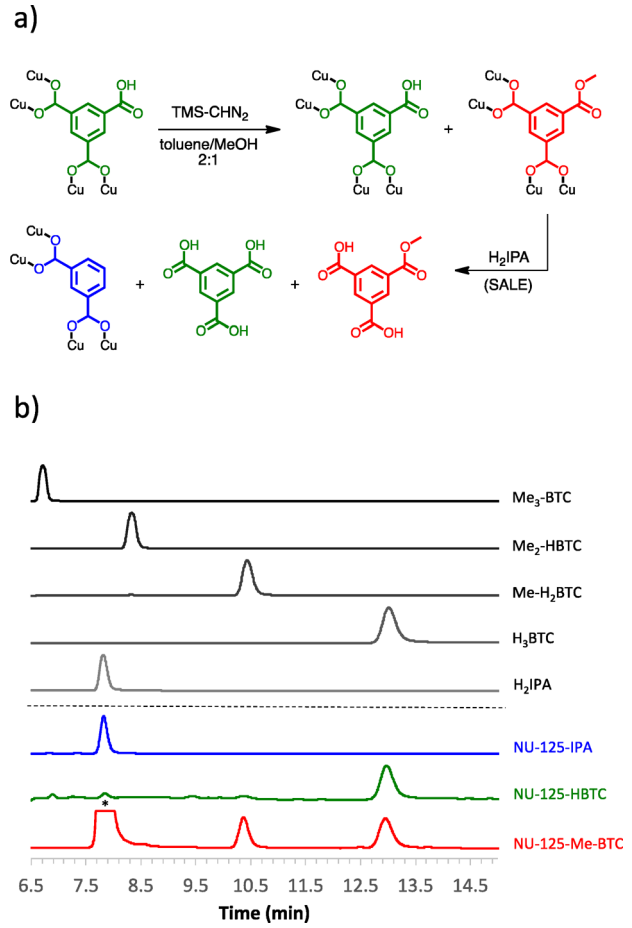

Figure 3. (a) Selective methylation of the **HBTC** unit inside the **NU-125-HBTC** framework and its subsequent extraction by SALE with **H_2IPA**. (b) HPLC analysis data. Elution profiles of the trimethyl ester of **H_3BTC**, the dimethyl ester of **H_3BTC**, and the monomethyl ester of **H_3BTC** as well as **H_3BTC** and **H_2IPA** (black). Elution profiles of the diacid linker extracted from **NU-125-IPA** (blue), the diacid linker extracted from **NU-125-HBTC** (green), and diacid linkers extracted from **NU-125-Me-BTC** (red). The peak marked with an asterisk (*) corresponds to excess **H_2IPA** from the SALE solution.

DOI: 10.1021/ic502697y
Inorg. Chem. 2015, 54, 1785−1790

support these assignments. Integration of the HPLC peaks shows that the extent of methylation is 40%.[49]

Notably, treatment of **NU-125-IPA** with the methylating agent under conditions identical to those used for **NU-125-HBTC** (2 equiv of TMS-CHN_2 at 0 °C in 2:1 toluene/MeOH solution for 24 h) resulted in no detectable methylation, as illustrated by ^{1}H NMR measurements (Figure S9, Supporting Information). PXRD measurements indicated that the crystallinity of the framework was again preserved, while N_2 sorption data for the crystals activated by supercritical CO_2 drying yielded a BET area of 2640 m^2/g, closely similar to that of samples that had not been exposed to TMS−CHN_2 (Figures S15 and S19, Supporting Information). Thus, the control experiments confirm the absence of free −COOH moieties in **NU-125-IPA** and further corroborate the model put forward by Barin et al. for defect incorporation into **NU-125**.

CONCLUSIONS

Desired free carboxylic acid moieties can be installed in a congener of **NU-125** featuring a high density of ditopic **IPA** units by exchanging these units for **HBTC**. The resulting product **NU-125-HBTC** is crystalline (isostructural with **NU-125**) and porous, and the presence of the noncoordinating carboxylic acid groups has been confirmed by DRIFTS. The −COOH groups are available for subsequent participation in chemical reaction, as demonstrated by postsynthesis methylation of the MOF with TMS−CHN_2 with retention of crystallinity and porosity. The results serve to further illustrate how SALE can enable incorporation of reactive (and thus challenging to install) chemical groups into MOFs.

ASSOCIATED CONTENT

Supporting Information

Experimental details, ^{1}H NMR, PXRD, N_2 sorption, and TGA data. This material is available free of charge via the Internet at http://pubs.acs.org.

AUTHOR INFORMATION

Corresponding Authors

*E-mail: stoddart@northwestern.edu.
*E-mail: j-hupp@northwestern.edu.
*E-mail: o-farha@northwestern.edu.

Author Contributions

The manuscript was written through contributions of all authors. All authors have given approval to the final version of the manuscript.

Notes

The authors declare no competing financial interest.

ACKNOWLEDGMENTS

Work in the Hupp/Farha lab was supported by the U.S. Department of Energy, Office of Basic Energy Sciences, Separations and Analysis program, award no. DE-FG02-12ER16362. P.Z.M. thanks the Army Research Office (grant W911NF-12-1-0130) for financial support. This work made use of Northwestern's CleanCat Core facility. The CleanCat Core facility acknowledges funding from the Department of Energy (DE-FG-02-03ER15457) used for the purchase of the Thermo Nicolet/Harrick DRIFTS system. This research is part (Project 34-944) of the Joint Center of Excellence in Integrated Nano-Systems (JCIN) at King Abdulaziz City for Science and Technology (KACST) and Northwestern University (NU). The authors would like to thank both KACST and NU for their continued support of this research.

REFERENCES

(1) Furukawa, H.; Cordova, K. E.; O'Keeffe, M.; Yaghi, O. M. *Science* **2013**, *341*, 974−986.
(2) He, Y.; Zhou, W.; Qian, G.; Chen, B. *Chem. Soc. Rev.* **2014**, *43*, 5657−5678.
(3) Farha, O. K.; Malliakas, C. D.; Kanatzidis, M. G.; Hupp, J. T. *J. Am. Chem. Soc.* **2009**, *132*, 950−952.
(4) Furukawa, H.; Ko, N.; Go, Y. B.; Aratani, N.; Choi, S. B.; Choi, E.; Yazaydin, A. Ö.; Snurr, R. Q.; O'Keeffe, M.; Kim, J.; Yaghi, O. M. *Science* **2010**, *329*, 424−428.
(5) Qiu, S.; Xue, M.; Zhu, G. *Chem. Soc. Rev.* **2014**, *43*, 6116−6140.
(6) Li, J.-R.; Sculley, J.; Zhou, H.-C. *Chem. Rev.* **2011**, *112*, 869−932.
(7) Wilmer, C. E.; Farha, O. K.; Bae, Y.-S.; Hupp, J. T.; Snurr, R. Q. *Energy Environ. Sci.* **2012**, *5*, 9849−9856.
(8) Lee, J.; Farha, O. K.; Roberts, J.; Scheidt, K. A.; Nguyen, S. T.; Hupp, J. T. *Chem. Soc. Rev.* **2009**, *38*, 1450−1459.
(9) Liu, J.; Chen, L.; Cui, H.; Zhang, J.; Zhang, L.; Su, C.-Y. *Chem. Soc. Rev.* **2014**, *43*, 6011−6061.
(10) Yoon, M.; Srirambalaji, R.; Kim, K. *Chem. Rev.* **2011**, *112*, 1196−1231.
(11) Kreno, L. E.; Leong, K.; Farha, O. K.; Allendorf, M.; Van Duyne, R. P.; Hupp, J. T. *Chem. Rev.* **2011**, *112*, 1105−1125.
(12) Barea, E.; Montoro, C.; Navarro, J. A. R. *Chem. Soc. Rev.* **2014**, *43*, 5419−5430.
(13) Katz, M. J.; Mondloch, J. E.; Totten, R. K.; Park, J. K.; Nguyen, S. T.; Farha, O. K.; Hupp, J. T. *Angew. Chem., Int. Ed.* **2014**, *53*, 497−501.
(14) Wang, J.-L.; Wang, C.; Lin, W. *ACS Catal.* **2012**, *2*, 2630−2640.
(15) So, M. C.; Jin, S.; Son, H.-J.; Wiederrecht, G. P.; Farha, O. K.; Hupp, J. T. *J. Am. Chem. Soc.* **2013**, *135*, 15698−15701.
(16) Son, H.-J.; Jin, S.; Patwardhan, S.; Wezenberg, S. J.; Jeong, N. C.; So, M.; Wilmer, C. E.; Sarjeant, A. A.; Schatz, G. C.; Snurr, R. Q.; Farha, O. K.; Wiederrecht, G. P.; Hupp, J. T. *J. Am. Chem. Soc.* **2012**, *135*, 862−869.
(17) Cohen, S. M. *Chem. Rev.* **2011**, *112*, 970−1000.
(18) Farha, O. K.; Hupp, J. T. *Acc. Chem. Res.* **2010**, *43*, 1166−1175.
(19) Farha, O. K.; Mulfort, K. L.; Thorsness, A. M.; Hupp, J. T. *J. Am. Chem. Soc.* **2008**, *130*, 8598−8599.
(20) Lalonde, M. B.; Getman, R. B.; Lee, J. Y.; Roberts, J. M.; Sarjeant, A. A.; Scheidt, K. A.; Georgiev, P. A.; Embs, J. P.; Eckert, J.; Farha, O. K.; Snurr, R. Q.; Hupp, J. T. *CrystEngComm* **2013**, *15*, 9408−9414.
(21) Mohideen, M. I. H.; Xiao, B.; Wheatley, P. S.; McKinlay, A. C.; Li, Y.; Slawin, A. M. Z.; Aldous, D. W.; Cessford, N. F.; Düren, T.; Zhao, X.; Gill, R.; Thomas, K. M.; Griffin, J. M.; Ashbrook, S. E.; Morris, R. E. *Nat. Chem.* **2011**, *3*, 304−310.
(22) Mu, B.; Li, F.; Walton, K. S. *Chem. Commun.* **2009**, 2493−2495.
(23) Custelcean, R.; Gorbunova, M. G. *J. Am. Chem. Soc.* **2005**, *127*, 16362−16363.
(24) Zhang, Q.; Yu, J.; Cai, J.; Song, R.; Cui, Y.; Yang, Y.; Chen, B.; Qian, G. *Chem. Commun.* **2014**, *50*, 14455−14458.
(25) Gadzikwa, T.; Farha, O. K.; Mulfort, K. L.; Hupp, J. T.; Nguyen, S. T. *Chem. Commun.* **2009**, 3720−3722.
(26) Kim, K. C.; Yu, D.; Snurr, R. Q. *Langmuir* **2013**, *29*, 1446−1456.
(27) Burnett, B. J.; Barron, P. M.; Hu, C.; Choe, W. *J. Am. Chem. Soc.* **2011**, *133*, 9984−9987.
(28) Kim, M.; Cahill, J. F.; Su, Y.; Prather, K. A.; Cohen, S. M. *Chem. Sci.* **2012**, *3*, 126−130.
(29) Karagiaridi, O.; Bury, W.; Sarjeant, A. A.; Stern, C. L.; Farha, O. K.; Hupp, J. T. *Chem. Sci.* **2012**, *3*, 3256−3260.
(30) Karagiaridi, O.; Lalonde, M. B.; Bury, W.; Sarjeant, A. A.; Farha, O. K.; Hupp, J. T. *J. Am. Chem. Soc.* **2012**, *134*, 18790−18796.
(31) Kim, M.; Cahill, J. F.; Fei, H.; Prather, K. A.; Cohen, S. M. *J. Am. Chem. Soc.* **2012**, *134*, 18082−18088.
(32) Takaishi, S.; DeMarco, E. J.; Pellin, M. J.; Farha, O. K.; Hupp, J. T. *Chem. Sci.* **2013**, *4*, 1509−1513.

DOI: 10.1021/ic502697y
Inorg. Chem. 2015, 54, 1785−1790

(33) Bury, W.; Fairen-Jimenez, D.; Lalonde, M. B.; Snurr, R. Q.; Farha, O. K.; Hupp, J. T. *Chem. Mater.* **2013**, *25*, 739−744.
(34) Fei, H.; Cahill, J. F.; Prather, K. A.; Cohen, S. M. *Inorg. Chem.* **2013**, *52*, 4011−4016.
(35) Li, T.; Kozlowski, M. T.; Doud, E. A.; Blakely, M. N.; Rosi, N. L. *J. Am. Chem. Soc.* **2013**, *135*, 11688−11691.
(36) Karagiaridi, O.; Bury, W.; Tylianakis, E.; Sarjeant, A. A.; Hupp, J. T.; Farha, O. K. *Chem. Mater.* **2013**, *25*, 3499−3503.
(37) Pullen, S.; Fei, H.; Orthaber, A.; Cohen, S. M.; Ott, S. *J. Am. Chem. Soc.* **2013**, *135*, 16997−17003.
(38) Karagiaridi, O.; Bury, W.; Mondloch, J. E.; Hupp, J. T.; Farha, O. K. *Angew. Chem., Int. Ed.* **2014**, *53*, 4530−4540.
(39) Deria, P.; Mondloch, J. E.; Karagiaridi, O.; Bury, W.; Hupp, J. T.; Farha, O. K. *Chem. Soc. Rev.* **2014**, *43*, 5896−5912.
(40) Morabito, J. V.; Chou, L.-Y.; Li, Z.; Manna, C. M.; Petroff, C. A.; Kyada, R. J.; Palomba, J. M.; Byers, J. A.; Tsung, C.-K. *J. Am. Chem. Soc.* **2014**, *136*, 12540−12543.
(41) Madrahimov, S. T.; Atesin, T. A.; Karagiaridi, O.; Sarjeant, A. A.; Farha, O. K.; Hupp, J. T.; Nguyen, S. T. *Cryst. Growth Des.* **2014**, *14*, 6320−6324.
(42) So, M. C.; Beyzavi, M. H.; Sawhney, R.; Shekhah, O.; Eddaoudi, M.; Al-Juaid, S. S.; Hupp, J. T.; Farha, O. K. *Chem. Commun.* **2015**, *51*, 85−88.
(43) Barin, G.; Krungleviciute, V.; Gutov, O.; Hupp, J. T.; Yildirim, T.; Farha, O. K. *Inorg. Chem.* **2014**, *53*, 6914−6919.
(44) Park, J.; Wang, Z. U.; Sun, L.-B.; Chen, Y.-P.; Zhou, H.-C. *J. Am. Chem. Soc.* **2012**, *134*, 20110−20116.
(45) Wilmer, C. E.; Farha, O. K.; Yildirim, T.; Eryazici, I.; Krungleviciute, V.; Sarjeant, A. A.; Snurr, R. Q.; Hupp, J. T. *Energy Environ. Sci.* **2013**, *6*, 1158−1163.
(46) Nelson, A. P.; Farha, O. K.; Mulfort, K. L.; Hupp, J. T. *J. Am. Chem. Soc.* **2008**, *131*, 458−460.
(47) Mondloch, J. E.; Karagiaridi, O.; Farha, O. K.; Hupp, J. T. *CrystEngComm* **2013**, *15*, 9258−9264.
(48) National Insitute of Standards and Technology. http://webbook.nist.gov/cgi/cbook.cgi?ID=C65850&Type=IR-SPEC&Index=2-IR-SPEC (accessed Sept 03, 2014).
(49) It should be noted that the extent of methylation was calculated based on the bulk amount of MOF sample used in the HPLC analysis and thus constitutes a statistical average. The extent of methylation may vary from crystallite to crystallite.

DOI: 10.1021/ic502697y
Inorg. Chem. 2015, 54, 1785−1790